Revista Mexicana de Astronomía y Astrofísica, **39**, 89–105 (2003)

LYNGÅ 1, A SMALL OPEN CLUSTER CONTAINING A RED-SUPERGIANT MEMBER[1]

R. A. Vázquez,[2,3] E. E. Giorgi,[3,4] M. A. Brusasco,[4] G. Baume,[2,3] and G. R. Solivella[3]

Received 2002 January 10; accepted 2003 March 10

RESUMEN

Presentamos observaciones fotométricas *CCD UBVRI* (sistema de Cousins) complementadas con observaciones espectróscopicas y polarimétricas en el cúmulo abierto Lyngå 1. Nuestros datos indican que el enrojecimiento del cúmulo es $E_{B-V} = 0.45 \pm 0.03$, que la razón $A_V/E_{B-V} = R$ sugiere que la ley de extinción puede ser ligeramente anómala ($R \approx 3.5$) y que su módulo de distancia es $V_0 - M_V = 11.40 \pm 0.2$. La edad de Lyngå 1 está comprendida entre 100 y 125 millones de años de acuerdo a un ajuste de isocronas teóricas y la pendiente del espectro de masas es $x \approx 1.7$. La estrella roja más brillante del campo es un miembro de este cúmulo, cuyo tipo espectral es K2 II–Ib.

ABSTRACT

We present CCD *UBVRI* (Cousins system) photometric observations complemented with spectroscopic and polarimetric observations that were carried out in the open cluster Lyngå 1. Our data indicate that the cluster reddening is $E_{B-V} = 0.45 \pm 0.03$, the ratio $A_V/E_{B-V} = R$ suggests that the extinction law may be slightly anomalous ($R \approx 3.5$) and that the cluster distance modulus is $V_0 - M_V = 11.40 \pm 0.2$. The age of Lyngå 1 is between 100 and 125 Myr according to a fitting of theoretical isochrones, and the slope of its mass spectrum is $x \approx 1.7$. The brightest red star in the field is a cluster member of spectral type K2 II–Ib.

Key Words: **OPEN CLUSTERS AND ASSOCIATIONS: INDIVIDUAL (LYNGÅ 1) — STARS: MASS FUNCTION, SPECTRAL CLASSIFICATION — STARS: POLARIZATION**

1. INTRODUCTION

The study of open clusters produces very valuable information that can be used to test not only star formation theories but also theories of the formation and kinematics of the galactic disk (Hron 1987; Phelps & Janes 1993, 1994; Carraro et al. 1994). Open clusters are also a main source of stellar enrichment; however, quite often they do not receive the necessary attention (mainly those of small size) since accurate and deep observations are needed to obtain a better estimate of their observational parameters.

Lyngå 1, C1356−619 ($\alpha_{2000} = 14^{\rm h}00^{\rm m}12^{\rm s}$, $\delta_{2000} = -62°11'32''$; $l = 310\overset{\circ}{.}86$, $b = -00\overset{\circ}{.}38$) is a very small open cluster (diameter $< 2'$) lying in the Centaurus OB1 association. Peterson & FitzGerald (1988; hereafter PF88) performed the only previous photometric study, using UBV photoelectric photometry for 24 stars down to $V \approx 15$ mag to derive its distance, reddening, and age. However, the presence of a red star in the cluster field, No. 14 in their notation, whose location in the cluster color-magnitude diagram, CMD, resembles that of an evolved cluster member, and the lack of a deep photometric study motivated us to include Lyngå 1 in our ongoing program of small open clusters. According to PF88, star No. 14 is not a cluster member. We want here not only to confirm the earlier findings of PF88 but also to extend their photometry to get more information on the lower main sequence structure, and to study

[1]Based on observations collected at the University of Toronto Southern Observatory, Las Campanas, Chile, and the Complejo Astronómico El Leoncito, Argentina, operated under agreement of CONICET and La Plata, Córdoba, and San Juan Universities.

[2]Member of the Carrera de Investigador Científico, CONICET.

[3]Facultad de Ciencias Astronómicas y Geofísicas de la UNLP, IALP-CONICET.

[4]Fellow of Comisión de Investigaciones Científicas de la Provincia de Buenos Aires Argentina.

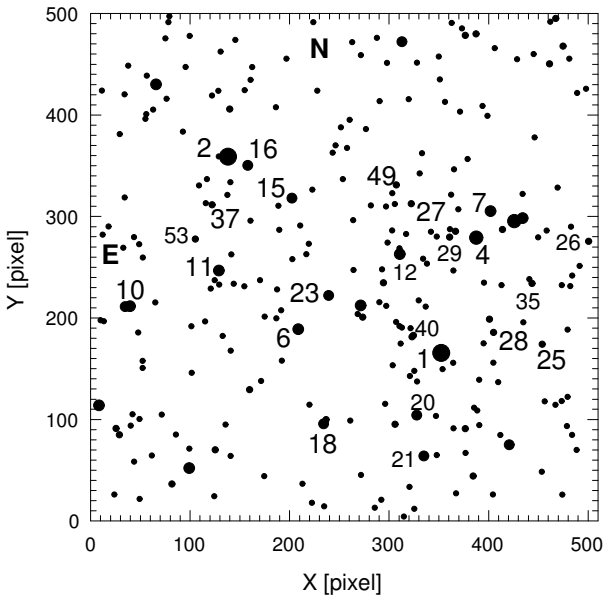

Fig. 1. The finding chart for Lyngå 1, covering 4′ on each side. The size of the symbols represents star magnitudes, approximately. Numbers are our identification of the stars observed by PF88. North and East are indicated.

the cluster mass function. Moreover, we decided to undertake a preliminary analysis of the interstellar medium properties towards Lyngå 1. So, with this goal in mind, we carried out *UBVRI* multicolor polarimetry of 16 stars in the cluster area too.

Section 2 describes the photometric observations and the data reduction process. In § 3 we discuss memberships, reddening, distance, age and special stars. The cluster mass function is also described in this section. Section 4 contains our preliminary findings from the polarimetric study, and the conclusions can be found in § 5.

2. PHOTOMETRIC OBSERVATIONS

The central part of Lyngå 1, as shown in the finding chart of Figure 1, was observed in the *UBVRI* filters (Cousins system) during an observing run on June 20, 1993, with the 60 cm telescope of the University of Toronto Southern Observatory, Las Campanas, Chile. The telescope was equipped with a PM 512 × 512 METHACROME-II UV-coated chip covering 4′ on a side (scale 0.45″ pixel^{-1}). To help the reader, we have indicated in Fig. 1 all the stars previously observed by PF88, but the numbering correponds to the present investigation.

The observations were carried out under good photometric conditions characterized by a mean seeing value of 1.2″. Details of the exposure times

TABLE 1

DETAILS OF THE EXPOSURE TIMES

	Exposure time (s)[a]	
Filter	Long	Short
U	1200(2)	···
B	700(2)	70
V	450(1)	50
R	110(2)	15
I	110(2)	10

[a]Number of observations in brackets.

TABLE 2

PHOTOMETRIC ERRORS AT DIFFERENT MAGNITUDE INTERVALS

V range	ϵ_V	ϵ_{B-V}	ϵ_{U-B}	ϵ_{V-R}	ϵ_{V-I}
≤ 14	0.021	0.026	0.036	0.022	0.021
14 to 16	0.021	0.028	0.050	0.023	0.022
16 to 17	0.025	0.041	0.090	0.028	0.030
17 to 19	0.039	0.076	···	0.044	0.046

are included in Table 1. In order to improve the statistics of faint stars, two long exposures per filter were obtained; unfortunately, during the data saving process one of the long V exposures was missing. CCD signatures were removed using bias and sky flat frames. Instrumental magnitudes and colors were derived using the point spread function method (Stetson 1987), and transformed to the standard system through two groups of secondary "standard stars" observed in the open cluster NGC 5606 (Vázquez et al. 1994). The accuracy of the transformation was 0.02 mag for V, $V-R$, and $V-I$, 0.03 for $B-V$ and 0.04 for $U-B$. Program and "standard" stars, including blue and red stars for an adequate spectral coverage, were all observed at air mass $\leq$ 1.3. Extinction coefficients, on the other hand, were taken from Grotues & Gocherman (1992). Calibration errors were quadratically added to DAOPHOT errors and are listed in Table 2 at different magnitude intervals. An estimation of the internal errors of our photometry was carried out from the comparison of magnitudes and color indices obtained at different exposure times (long and short), except for the $U-B$ index, where we could only compare two long exposures. These comparisons indicated that our internal errors are better than 0.02 mag in colors and magnitudes. Hereafter, we will assume that the range of useful

TABLE 3

CCD PHOTOMETRIC OBSERVATIONS IN LYNGÅ 1

No.	PF88	X	Y	V	$(B-V)$	$(U-B)$	$(V-R)$	$(V-I)$	Notes
1	14	352.42	165.46	10.57	1.65	2.19	1.01	2.40	a, b, lm
2	5	138.10	358.87	10.96	0.11	0.19	0.07	0.18	a
3		425.84	295.34	11.05	0.33	−0.09	0.25	0.62	*, lm
4	20	387.61	279.08	11.59	0.49	0.11	0.33	0.75	a
5		271.43	212.26	12.07	0.32	−0.08	0.22	0.54	a, *, lm
6	8	208.72	188.89	12.39	0.26	0.24	0.16	0.39	
7	19	401.94	305.15	12.44	0.32	−0.04	0.23	0.59	*, lm
8		99.15	52.03	12.49	1.34	1.69	0.84	1.96	
9		434.22	298.36	12.53	0.27	0.23	0.16	0.38	a, b
10	1	39.67	211.56	12.59	0.41	0.33	0.27	0.63	
11	2	128.97	246.69	12.63	2.31	0.88	1.54	3.79	
12	22	310.81	262.91	12.83	0.33	0.05	0.23	0.58	*, lm
13		8.51	113.85	12.93	2.12	1.15	1.38	3.37	
14		65.84	430.12	12.95	1.67	0.37	1.14	2.86	
15	7	202.32	318.03	13.04	0.34	−0.02	0.25	0.62	*, lm
16	6	158.00	350.32	13.14	0.32	0.27	0.23	0.55	pm
17		420.76	75.00	13.44	1.31	1.43	0.80	1.89	
18	10	234.26	95.62	13.47	0.41	0.10	0.28	0.70	*, lm
19		34.83	211.11	13.94	0.69	0.35	0.47	1.14	pm
20	12	327.82	104.17	13.94	0.41	0.22	0.27	0.69	*, lm
21	11	334.96	63.99	13.97	0.61	0.20	0.39	0.91	
22		312.92	472.08	13.99	0.74	0.46	0.48	1.06	
23	9	239.32	222.16	13.99	0.36	0.24	0.23	0.58	*, lm
24		376.64	478.39	14.06	0.51	0.24	0.34	0.89	pm
25	16	453.92	174.08	14.20	0.45	0.32	0.28	0.70	*, lm
26	18	500.52	275.42	14.23	0.56	0.41	0.46	0.98	pm
27	23	322.36	312.51	14.31	0.53	0.38	0.34	0.85	pm
28	15	405.03	185.68	14.38	1.43	1.27	0.90	2.19	b
29	21	360.84	279.58	14.45	0.77	0.38	0.51	1.20	b
30		400.92	198.67	14.48	0.44	0.36	0.28	0.71	pm
31		467.54	495.11	14.52	0.53	0.32	0.33	0.85	pm
32		159.86	129.27	14.80	0.74	0.26	0.49	1.20	pm
33		81.81	36.35	14.88	2.17	0.32	1.56	3.96	
34		273.56	200.78	14.89	0.93	0.20	0.65	1.42	
35	17	443.66	233.99	14.94	0.66	0.37	0.43	1.08	b, pm
36		29.04	84.79	15.02	0.63	0.25	0.42	0.98	pm
37	4	122.14	311.49	15.03	1.29	0.20	0.90	2.25	
38		461.24	450.32	15.03	1.04	0.73	0.66	1.58	
39		125.24	70.02	15.03	1.30	1.02	0.87	2.10	
40	13	324.49	182.76	15.04	0.82	0.26	0.52	1.22	b, pm
41		366.77	285.31	15.17	0.64	0.22	0.45	1.06	pm
42		306.01	95.21	15.35	1.89	1.10	1.23	2.99	

TABLE 3 (CONTINUED)

No.	PF88	X	Y	V	$(B-V)$	$(U-B)$	$(V-R)$	$(V-I)$	Notes
43		323.07	181.33	15.41	0.74	0.39	0.51	1.21	pm
44		376.64	90.83	15.45	1.22	1.24	0.76	1.72	
45		294.39	234.61	15.49	0.97	0.48	0.63	1.52	pm
46		236.72	99.75	15.49	0.87	0.57	0.56	1.34	
47		413.96	287.08	15.55	0.64	0.20::	0.42	1.04	pm
48		139.88	405.74	15.58	0.83	0.50	0.55	1.24	
49	24	307.35	331.02	15.61	0.71	0.12	0.45	1.10	b
50		25.69	91.11	15.72	0.78	0.38	0.52	1.31	pm
51		387.39	479.81	15.76	0.79	0.52	0.50	1.31	
52		384.53	44.14	15.81	0.79	0.25	0.50	1.20	pm
53	3	105.32	277.67	15.92	0.78	0.31	0.51	1.21	pm
54		474.91	467.72	15.96	0.81	0.27	0.51	1.20	pm
55		371.36	403.23	16.00	1.53	0.65	1.05	2.65	
56		132.76	182.18	16.03	1.01	0.33	0.65	1.63	pm
57		353.68	149.50	16.04	0.90	0.47	0.65	1.60::	pm
58		37.81	448.56	16.13	0.88	0.48	0.56	1.35	pm
59		71.47	104.68	16.16	2.05::	0.59::	1.46	3.52	
60		101.68	145.93	16.17	0.94	0.92	0.63	1.43	
61		311.63	174.73	16.18	1.13	0.75	0.74	1.85	
62		196.89	455.43	16.19	0.93	0.60	0.63	1.55	pm
63		409.65	136.74	16.21	1.06	0.54	0.70	1.72	pm
64		474.15	25.92	16.31	0.85	0.60	0.61	1.36	
65		365.29	346.40	16.33	0.88	0.50	0.58	1.34	pm
66		310.48	191.99	16.33	0.91	0.54	0.62	1.45	pm
67		481.08	455.35	16.38	0.84	0.36	0.57	1.44	pm
68		124.33	24.34	16.39	1.15	0.93	0.76	1.98	
69		128.80	359.02	16.46	0.89::		0.59	1.52	pm
70		216.87	262.74	16.49	1.07	0.78	0.72	1.74	
71		440.97	238.24	16.52	1.27	0.87::	0.90	2.03	
72		95.49	447.23	16.56	1.45		0.96	2.33	
73		378.93	356.55	16.58	0.85	0.24	0.55	1.38	pm
74		34.30	318.69	16.58	1.07	0.59	0.72	1.78	pm
75		362.94	490.61	16.61	1.27	0.88::	0.83	2.19	
76		212.93	36.55	16.63	1.21	0.70	0.81	2.08	
77		320.52	33.47	16.63	1.45	0.93::	1.22	3.64	
78		449.86	279.42	16.66	0.84	0.49	0.57	1.41	
79		101.36	191.73	16.72	1.24	0.93::	0.83	2.02	
80		320.91	142.68	16.73	0.99	0.30	0.70	1.81	pm
81		292.97	247.82	16.74	1.37	0.94::	0.97	2.43	
82		135.61	94.86	16.74	1.14	0.92::	0.71	1.87	
83		141.45	262.51	16.76	1.05	1.10::	0.70	1.68	
84		376.79	66.97	16.78	0.86	0.19	0.58	1.43	
85		412.96	232.27	16.82	0.93	0.52::	0.63	1.55	pm

TABLE 3 (CONTINUED)

No.	PF88	X	Y	V	$(B-V)$	$(U-B)$	$(V-R)$	$(V-I)$	Notes
86		140.54	333.70	16.86	0.81	0.27	0.54	1.30	pm
87		406.25	465.75	16.89	1.03	0.31	0.66	1.65	pm
88		310.40	268.57	16.90	1.20		0.78	2.04	pm
89		461.97	491.77	16.95	0.98	0.77::	0.60	1.41	
90		347.93	64.82	16.95	2.19		1.45	3.56	
91		347.15	103.36	16.96	0.90	0.57	0.65	1.56	
92		219.28	273.02	16.97	1.54		1.08	2.93	
93		482.11	231.37	16.99	0.94	0.31::	0.61	1.44	pm
94		478.75	93.40	17.01	1.00	0.38::	0.70	1.69	pm
95		120.77	228.90	17.01	1.25	0.65::	0.90	2.25	pm
96		162.38	447.12	17.01	1.33	0.76	0.91	2.32	
97		143.82	233.61	17.02	0.91	0.43	0.61	1.54	
98		329.72	217.27	17.02	0.91	0.18::	0.61	1.51	
99		482.89	289.90	17.04	0.89	0.42	0.62	1.51	
100		227.89	423.84	17.06	1.04	0.61::	0.65	1.63	pm
101		154.92	424.38	17.11	1.46	0.50::	0.99	2.57	
102		336.83	211.07	17.11	0.95	0.55::	0.65	1.57	pm
103		312.88	190.48	17.13	1.15		0.77	1.69	pm
104		99.58	477.86	17.18	1.08	0.63::	0.67	1.62	pm
105		34.18	420.22	17.25	1.15	1.64::	0.76	1.89	
106		222.46	17.85	17.27	1.39	0.40::	0.97	2.41	
107		303.05	286.19	17.27	2.15	0.39::	1.58	3.96	
108		12.17	282.01	17.28	1.06	0.95::	0.62	1.46	
109		362.33	321.43	17.31	1.15	0.67::	0.77	1.96	pm
110		10.05	197.65	17.33	1.00	0.74::	0.65	1.48	
111		398.87	399.09	17.36	1.51		1.05	2.66	
112		85.72	85.03	17.38	1.83		1.23	3.15	
113		117.02	336.70	17.39	0.85	0.39	0.60	1.54	
114		109.01	330.51	17.41	0.92	0.60::	0.62	1.52	
115		298.42	274.23	17.44	1.11	1.65::	0.74	1.72	
116		271.77	45.25	17.44	1.31	1.95::		2.13	
117		56.52	438.69	17.44	1.28		0.79	1.92	pm
118		234.77	14.37	17.44	1.02	0.54::	0.63	1.59	pm
119		469.33	328.37	17.47	1.26		0.85	2.03	pm
120		115.18	196.54	17.50	1.15	0.75::	0.74	1.86	pm
121		296.13	115.30	17.50	1.07	1.03::	0.65	1.50	
122		55.11	396.12	17.50	1.03	0.71::	0.63	1.49	pm
123		364.46	155.72	17.56	1.07	1.23::	0.90	2.10	
124		219.98	114.49	17.56	1.25		0.81::	2.10::	pm
125		394.94	174.86	17.58	1.03	0.70::	0.66	1.69	pm
126		186.32	407.51	17.60	1.06		0.70	1.71	pm
127		171.42	137.90	17.61	0.99	0.13::	0.69	1.66	
128		174.52	44.07	17.62	1.07		0.73	1.65	pm

TABLE 3 (CONTINUED)

No.	PF88	X	Y	V	$(B-V)$	$(U-B)$	$(V-R)$	$(V-I)$	Notes
129		49.20	100.42	17.63	1.15		0.75	1.86	pm
130		488.96	421.60	17.64	1.82		1.25	3.24	
131		281.73	310.84	17.68	5.58::	−2.33::	1.42	2.77::	
132		268.39	203.75	17.69	0.89		0.71	1.77	
133		145.48	473.92	17.72	1.14	0.70::	0.66	1.86	pm
134		338.11	253.45	17.74	1.21		0.79	2.06	pm
135		130.71	462.40	17.78	1.18		0.82	1.88	pm
136		296.90	309.76	17.79	1.02	0.55::	0.63	1.62	
137		305.82	312.13	17.80	1.69		1.07	2.75	
138		29.26	381.07	17.81	1.45	0.20::	0.89	2.33	
139		479.38	188.44	17.82	1.01		0.68	1.59	
140		290.46	413.60	17.82	1.33	0.70::	0.80	2.12	pm
141		373.31	485.28	17.84	1.15		0.72	1.87	pm
142		154.50	231.06	17.86	1.12		0.79	1.96	pm
143		434.14	322.08	17.95	1.25		0.91	2.38	pm
144		13.34	196.69	17.98	1.23		0.83	1.91	pm
145		297.14	211.83	18.00	1.06	2.58::	0.83	1.95	
146		285.61	13.01	18.03	1.15		0.75	1.81	pm
147		49.27	21.66	18.05	1.43	1.57::	0.90	2.28	
148		210.64	291.00	18.08	0.90		0.62	1.54	
149		334.16	258.26	18.09	1.46		1.00	2.55	pm
150		260.36	395.12	18.13	1.42		0.98	2.44	pm
151		264.23	247.21	18.13	0.88	0.53::	0.69	1.68	
152		349.99	457.50	18.14	1.15		0.79	1.99	pm
153		297.89	451.28	18.14	1.64::		1.10	2.92	
154		170.29	237.12	18.16	1.20		0.80	1.87	pm
155		263.96	296.33	18.16	1.13		0.70	1.70	pm
156		303.15	322.88	18.18	0.95		0.80	1.87	
157		52.50	259.49	18.21	1.48		1.02	2.59	pm
158		257.75	367.38	18.24	1.35		0.95	2.32	pm
159		361.14	287.40	18.24	1.54		1.05	2.85	pm
160		287.78	475.90	18.25	1.49		0.99	2.53	pm
161		43.63	279.54	18.25	1.33		0.88	2.16	pm
162		52.27	150.64	18.27	1.10		0.73	1.93	
163		174.94	201.25	18.29	1.01		0.72	1.72	
164		390.57	138.98	18.30	1.88		1.30	3.17	
165		333.07	362.20	18.32	1.09		0.79	1.98	
166		253.51	336.76	18.37	1.32		0.91	2.30	pm
167		188.76	310.51	18.38	1.18		0.85	2.13	pm
168		325.38	147.84	18.38	1.31		0.87	1.96	pm
169		290.20	215.43	18.39	1.15		0.83	2.16	
170		317.16	282.61	18.40	1.30		0.86	2.16	pm
171		61.61	64.41	18.40	1.87		1.22	3.06	

TABLE 3 (CONTINUED)

No.	PF88	X	Y	V	$(B-V)$	$(U-B)$	$(V-R)$	$(V-I)$	Notes
172		191.53	207.52	18.42	1.34		1.02	2.28	pm
173		78.21	491.34	18.45	1.18		0.75	1.91	pm
174		367.29	27.13	18.48	1.19		0.79	1.97	pm
175		40.34	93.84	18.48	2.27		1.51	3.95	
176		328.04	451.42	18.50	1.23		0.81	2.01	pm
177		47.88	185.62	18.51	1.04		0.74	1.88	
178		99.25	71.22	18.53	1.37		0.73	1.93	pm
179		434.95	195.65	18.56	2.04		1.24	3.01	
180		488.42	69.96	18.56	1.68		1.08	2.70	pm
181		411.85	84.64	18.57	1.40		0.88	2.13	pm
182		467.24	114.38	18.59	1.08		0.64	1.79	
183		321.53	189.78	18.59	1.00		0.80	1.86	
184		11.35	423.94	18.61	1.77	0.69::	1.21	3.15	
185		137.47	321.18	18.62	1.26		0.90	2.30	pm
186		187.45	228.01	18.63	1.45		0.93	2.49	pm
187		48.83	272.64	18.63	1.19::		0.76	1.83	
188		160.68	295.79	18.65	1.44		0.98	2.46	pm
189		328.16	137.32	18.65	1.55		1.08	2.66	pm
190		445.30	459.99	18.65	1.40		0.95	2.40	pm
191		307.05	195.97	18.66	2.08		1.24	3.29	
192		404.37	26.03	18.66	1.71		1.07	2.71	
193		243.32	362.77	18.66	2.05		1.43	3.64	
194		115.75	313.01	18.66	1.36:		0.92	2.37	pm
195		364.59	246.66	18.66	1.13		0.70	1.81	
196		479.35	122.17	18.66	1.07		0.88	1.84	
197		319.75	415.45	18.67	1.60		0.97	2.51	pm
198		140.75	64.00	18.72	1.26		0.75	1.91	pm
199		483.99	241.67	18.75	1.43		0.71	1.83	pm
200		186.67	199.61	18.77	1.19		0.85	2.09	
201		385.42	111.52	18.77	1.56		1.04	2.61	pm
202		456.35	117.75	18.77	1.52	−0.01::	0.98	2.63	
203		314.84	4.32	18.78	1.22		0.81	1.93	
204		79.17	497.17	18.80	1.66		1.40	3.57	pm
205		192.17	157.86	18.84	1.28		0.72	1.86	pm
206		62.85	405.18	18.86	1.56::		0.91	2.56	pm
207		393.90	408.80	18.86	1.30		0.97	2.45	pm
208		18.09	290.05	18.87	1.27		0.79	1.93	pm
209		223.80	491.37	18.88	1.18		0.86	2.03	
210		473.51	232.26	18.95	1.34		0.91	2.22	pm
211		55.96	400.73	18.96	1.71::		1.18	2.83	pm
212		303.66	153.33	18.96	1.58		0.86	2.02	pm
213		364.70	91.20	19.00	1.24	1.37::	0.82	1.93	
214		390.62	94.31	19.01	1.26::		0.84	2.08	

TABLE 3 (CONTINUED)

No.	PF88	X	Y	V	$(B-V)$	$(U-B)$	$(V-R)$	$(V-I)$	Notes
215		251.60	387.78	19.02	1.37::	−0.32::	1.03	2.38	
216		65.06	215.19	19.02	1.33::	−2.17::	0.91	2.32	
217		428.63	454.84	19.10	1.60::		0.87	2.48	pm
218		342.12	284.87	19.11	1.49::		0.99	2.53	pm
219		369.59	307.00	19.13	1.13::		1.02	2.35	
220		325.34	11.92	19.15	1.89::		1.43	3.48	pm
221		395.43	234.74	19.17	1.46		0.91	2.09	pm
222		388.62	108.77	19.24	1.34		0.85	2.00	pm
223		347.86	280.12	19.24	0.36::		0.79	2.30	
224		129.32	232.76	19.25	1.78::		1.27::		pm
225		446.29	377.78	19.25	1.07::		0.91	2.04::	
226		43.73	58.36	19.26	1.48::		1.02	2.12	pm
227		222.84	326.32	19.26	−1.61::		1.28	4.28	
228		140.78	167.69	19.29	1.28::		0.91	2.19	
229		260.95	98.77	19.29	1.23::		1.03	2.36::	
230		351.03	434.93	19.32	1.60::		1.09	2.72	pm
231		262.94	471.71	19.35	1.68::		1.09	2.80	pm
232		473.42	118.11	19.40	3.42::		1.25	2.90::	
233		356.17	412.86	19.40::	1.24::	0.79::	0.94	2.21	
234		160.76	434.51	19.40	1.79::		1.12	2.66	pm
235		32.82	269.12	19.44	1.63::		0.89	2.22::	pm
236		92.78	383.56	19.45	1.17::		1.04	2.54	
237		404.76	155.84	19.47	1.24::		0.86	2.12::	
238		330.68	342.34	19.48	1.40::		1.13	2.58::	pm
239		124.76	237.10	19.48	1.44::		1.32::	4.02	pm
240		202.79	257.91	19.50	1.33::		0.82	2.01	
241		271.71	458.92	19.52	1.41::		0.84	2.17	pm
242		76.38	415.87	19.52	1.48::		1.03	2.45	pm
243		189.68	286.79	19.53	1.80::		1.12	2.61	pm
244		42.14	105.04	19.54	1.48::		1.02	2.63	pm
245		458.34	286.08	19.57	0.74::		0.77	2.01	
246		453.46	48.46	19.61	1.82::		1.11	2.90::	pm
247		23.87	25.99	19.63	1.44::		0.78	1.96::	
248		52.33	157.63	19.69::	1.42::		1.06::	2.68	pm
249		483.89	84.68	19.69	1.13::		1.01	2.28::	
250		497.95	425.71	19.74	1.88::		1.03	2.61::	pm
251		75.16	475.41	19.76	1.21::		0.97::	2.24::	
252		491.53	251.22	19.76::	1.70::		1.25::	2.90::	pm
253		128.40	423.78	19.80::	1.74::	0.01::	0.97::	2.53	
254		246.16	370.00	19.83	1.43::		1.08	2.54	
255		122.10	419.10	19.96	0.93::		1.17	2.82	
256		276.72	386.08	20.02::	0.99::		1.20::	2.65::	
257		292.23	20.81	22.23::	3.09::				

NOTES TO TABLE 3

(*) denotes stars used to derive the $E(B-V)$ mean color excess; (lm) denotes likely member stars; (pm) denotes probable member; Double colon (::) for photometric errors ≥ 0.10.

Stars with proper motions (in mas/y) available from ESA (1997):

Star 1: $\mu_\alpha cos\delta = -4.5$, $\mu_\delta = 2.8$;
Star 2: $\mu_\alpha cos\delta = -8.3$, $\mu_\delta = 0.2$;
Star 4: $\mu_\alpha cos\delta = -13.2$, $\mu_\delta = -10.2$;
Star 5: $\mu_\alpha cos\delta = -15.0$, $\mu_\delta = 4.9$;
Star 9: $\mu_\alpha cos\delta = -5.8$, $\mu_\delta = -5.3$;

Stars showing large differences with PF88:

Star 1:	$\Delta V = 0.17$;	$V_{\rm int} = 12.56$;	$\Delta V_{\rm int} = 0.10$;
Star 10:	$\Delta V = 0.18$;	$V_{\rm int} = 12.32$;	$\Delta V_{\rm int} = -0.09$;
Star 28:	$\Delta V = -0.46$;	$V_{\rm int} = 13.68$;	$\Delta V_{\rm int} = 0.24$;
Star 29:	$\Delta V = 0.56$;	$V_{\rm int} = 13.97$;	$\Delta V_{\rm int} = 0.08$;
Star 35:	$\Delta V = 0.14$;	$V_{\rm int} = 14.71$;	$\Delta V_{\rm int} = 0.07$;
Star 40:	$\Delta V = 0.89$;	$V_{\rm int} = 14.45$;	$\Delta V_{\rm int} = 0.30$;
Star 49:	$\Delta V = -1.21$;	$V_{\rm int} = 15.39$;	$\Delta V_{\rm int} = -0.99$;

photometric data includes only stars with errors < 0.10 mag. So, according to Table 2, good $U-B$ data are expected for stars with $V < 17$, while for other indices and V magnitude useful data go down to $V < 19$. The final photometric catalogue containing the star numbering, x and y coordinates, magnitudes and colors for 257 stars is shown in Table 3, together with the cross-references to the PF88 numbering.

Twenty four stars were observed by PF88; a comparison of their data with ours, in the sense CCD-PF88 data yielded mean differences and standard deviations of:

$$\langle \Delta V \rangle = -0.06 \pm 0.14,$$
$$\langle \Delta (B-V) \rangle = 0.07 \pm 0.04,$$
$$\langle \Delta (U-B) \rangle = 0.09 \pm 0.08.$$

Depite the fact that stars No. 1, 11, 28, 29, 40, and 49 were discarded before computing these values (since they show magnitude and color discrepancies larger than 0.4), the mean differences between CCD and photoelectric measures and deviations remain large. To investigate the origin of such differences we simulated a $16''$ aperture diaphragm around the stars showing the largest differences so as to obtain the integrated magnitudes, $V_{\rm int}$, of all companion stars found inside the aperture. The resulting integrated star magnitudes were compared with the photoelectric measures from PF88. At the bottom of Table 3 we give details showing that the $\Delta V_{\rm int}$ differences with PF88 are substantially reduced in most cases. In fact, except for two stars, all of them have positive of $\Delta V_{\rm int}$ values (as expected from using PSF method in crowded zones) and improvements are made in the sense that the large aperture photometry is just bringing the differences ΔV closer to zero. The two stars with negative differences, No. 28 (PF88 15) and No. 49 (PF88 24) are not significant: PF88 estimated an error of 0.11 mag for their star 15 (the highest error in their data set), while for their star 24 they gave no error estimation, since they have only one measurement (but one should notice that it is their faintest star, $V = 14.4$). The integrated magnitudes demonstrate that using a large aperture diaphragm in a moderately crowded field can produce the differences we have found. We do not, however, exclude the possibility that another explanation for the difference between PF88 and us could be a real discrepancy between the zero point of each study (it would affect both works). Whatever the cause, after the drastic reduction by using $V_{\rm int}$, we still see differences with some PF88 stars which can be attributed to undetected variability.

3. DATA ANALYSIS

3.1. *Membership*

Some recent information on proper motions in the area Lyngå 1 can be found for stars Nos. 1, 2, 4,

TABLE 4

POLARIZATION MEASUREMENTS

No.	Filter	P_λ	θ_λ	n	No.	Filter	P_λ	θ_λ	n
8	U	2.23 ± 1.39	75.95 ± 17.86	4	21	U	2.13 ± 0.63	78.98 ± 8.47	4
	B	1.13 ± 0.06	84.56 ± 1.52	4		B	0.5 ± 0.3	39.89 ± 17.19	4
	V	1.04 ± 0.03	84.85 ± 0.83	4		V	0.31 ± 0.23	10.67 ± 21.26	4
	R	0.95 ± 0.03	84.76 ± 0.90	4		R	0.1 ± 0.08	23.09 ± 22.92	4
	I	1.11 ± 0.08	83.51 ± 2.06	4		I	0.33 ± 0.34	38.18 ± 29.52	4
17	U				18	U	1.18 ± 0.23	60.58 ± 5.58	4
	B	1.12 ± 0.28	72.77 ± 7.16	4		B	0.89 ± 0.19	73.13 ± 6.12	4
	V	0.64 ± 0.05	73.97 ± 2.24	4		V	1.03 ± 0.13	63.53 ± 3.62	4
	R	0.64 ± 0.04	86.33 ± 1.79	4		R	1.15 ± 0.05	62.18 ± 1.25	4
	I	0.54 ± 0.09	88 ± 4.77	4		I	0.78 ± 0.13	67.87 ± 4.77	4
1	U	2.22 ± 1.97	165.05 ± 25.42	4	25	U	3.52 ± 1.2	55.42 ± 9.77	4
	B	0.87 ± 0.09	66 ± 2.96	4		B	1.33 ± 1.07	69.75 ± 23.05	4
	V	0.79 ± 0.08	62.52 ± 2.90	4		V	0.63 ± 0.45	57.54 ± 20.46	4
	R	0.83 ± 0.04	60.3 ± 1.38	4		R	0.95 ± 0.45	43.6 ± 13.57	4
	I	0.76 ± 0.06	63.04 ± 2.26	4		I	1.7 ± 0.79	19.73 ± 13.31	4
6	U	1.31 ± 0.19	82.66 ± 4.16	4	10	U	1.59 ± 0.19	91.01 ± 3.42	4
	B	1.61 ± 0.08	77.81 ± 1.42	4		B	1.05 ± 0.12	80.51 ± 3.27	4
	V	1.53 ± 0.07	82.96 ± 1.31	4		V	1.05 ± 0.09	71.56 ± 2.46	4
	R	1.52 ± 0.06	82.08 ± 1.13	4		R	1.11 ± 0.07	76.29 ± 1.81	4
	I	1.79 ± 0.12	82.26 ± 1.92	4		I	0.42 ± 0.15	76.35 ± 10.23	4
23	U				11	U	15.96 ± 4.5	81.14 ± 8.08	4
	B	70.84 ± 3.9	6.36 ± 1.58	2		B	1.94 ± 0.54	90.58 ± 7.97	4
	V	2.36 ± 1.25	66.53 ± 15.17	4		V	1.65 ± 0.06	83.62 ± 1.04	4
	R	15.52 ± 2.78	57.4 ± 5.13	4		R	1.71 ± 0.06	84.79 ± 1.01	4
	I	1.7 ± 2.89	58.17 ± 48.71	4		I	1.47 ± 0.08	88.24 ± 1.56	4
4	U	0.36 ± 0.57	99.77 ± 45.36	4	7	U	1.39 ± 0.22	68.54 ± 4.53	4
	B	0.6 ± 0.2	50.34 ± 9.55	4		B	0.85 ± 0.11	58.64 ± 3.71	4
	V	0.29 ± 0.08	69.5 ± 7.90	4		V	1.2 ± 0.45	50.11 ± 10.74	4
	R	0.3 ± 0.09	84.27 ± 8.59	4		R	1.09 ± 0.39	59.16 ± 10.25	4
	I	0.29 ± 0.09	40.43 ± 8.89	4		I	1.79 ± 0.75	41.49 ± 12.00	4
37	U	3.58 ± 0.39	159.24 ± 3.12	4	15	U	1.36 ± 0.19	64.94 ± 4.00	4
	B	1.22 ± 0.46	53.91 ± 10.80	4		B	0.78 ± 0.22	66.84 ± 8.08	4
	V	3.69 ± 0.69	62.49 ± 5.36	4		V	1.47 ± 0.17	73.26 ± 3.31	4
	R	5.13 ± 1.38	66.15 ± 7.71	4		R	1.32 ± 0.16	69.28 ± 3.47	4
	I	6.35 ± 1.35	64.71 ± 6.09	4		I	1.38 ± 0.32	65.96 ± 6.64	4
16	U	1.71 ± 0.28	74.23 ± 4.69	4	2	U	0.55 ± 0.12	61.33 ± 6.25	4
	B	2.12 ± 0.6	76.46 ± 8.11	4		B	0.61 ± 0.11	44.17 ± 5.17	4
	V	2.22 ± 0.62	93.76 ± 8.00	4		V	0.5 ± 0.1	49.39 ± 5.73	4
	R	2.17 ± 0.75	82.77 ± 9.90	4		R	0.43 ± 0.09	47.91 ± 6.00	4
	I					I	0.46 ± 0.1	47.98 ± 6.23	4

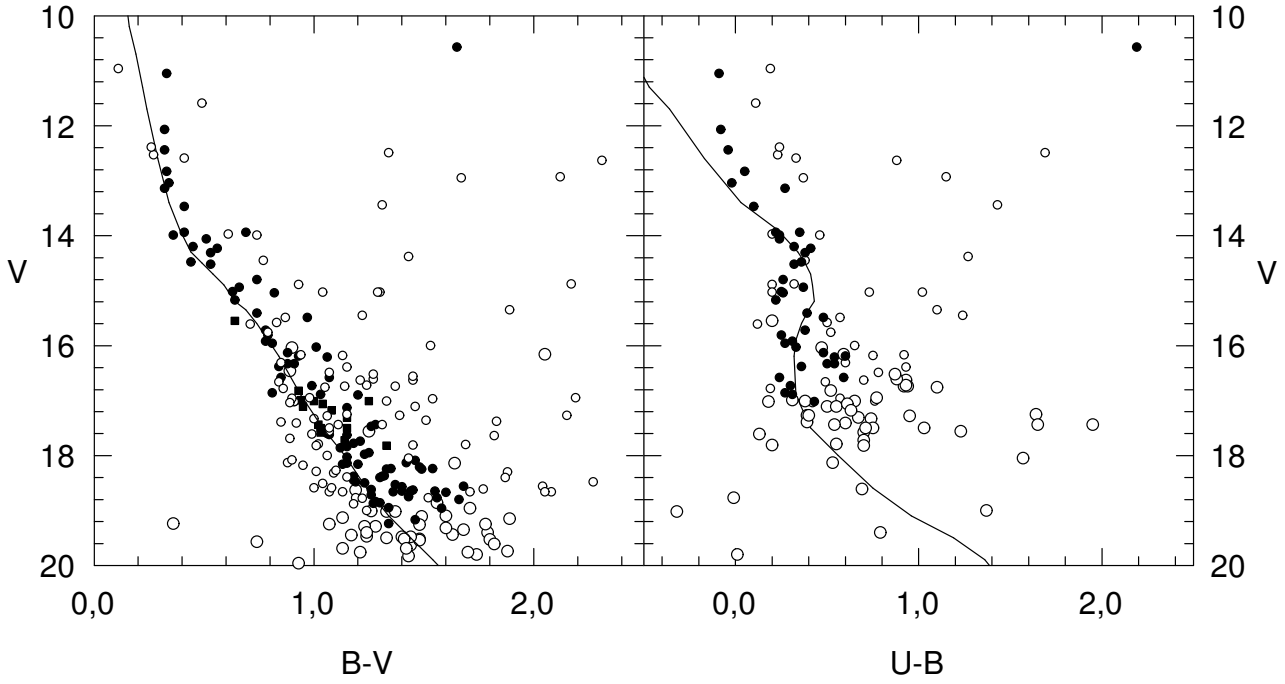

Fig. 2. The CMDs ($B-V$, V) and ($U-B$, V) of all stars observed in Lyngå 1. Filled circles denote likely and probable members; small open circles are non-members; large open circles are stars with errors larger than 0.10. Filled squares are probable member stars with no $U-B$ or unrealistic measures. The solid line is the Schmidt-Kaler (1982) ZAMS fitted to an apparent distance modulus of 12.8 (from visual absorption A_V and distance-corrected modulus given in § 3.3).

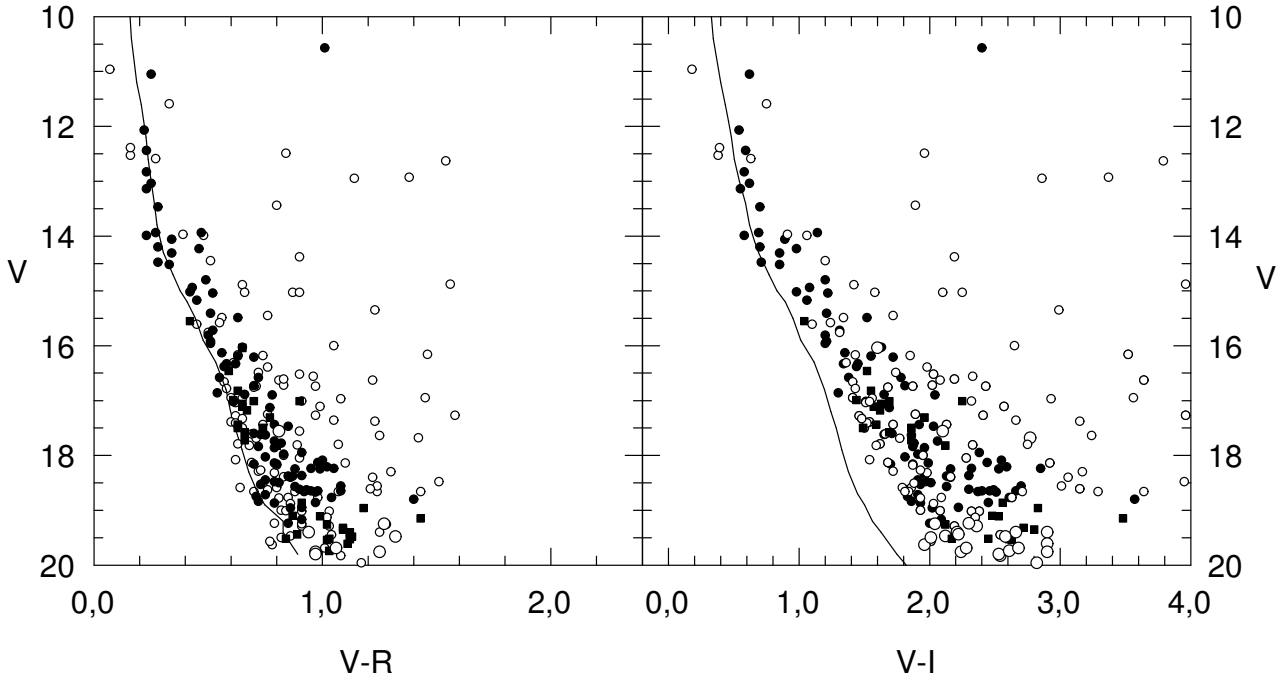

Fig. 3. The CMDs ($V-R$, V) and ($V-I$, V). Symbols as in Fig. 2. Solid lines are the ZAMS (Cousins 1978) fitted to an apparent distance modulus of 12.8. Notice the poor fit among faint stars in the ($V-I$, V) diagram.

5, and 9 in the Tycho 2 Catalogue (ESA 1997). This information, included at the bottom of Table 3, is insufficient to estimate membership in all the cluster, but it will help us in a couple of cases.

Figures 2, 3, and 4 are the two-color, TCD, and CMD photometric diagrams of Lyngå 1. In Figs. 2 and 3, the Schmidt-Kaler (1982) ZAMS has been fitted to an apparent distance modulus of 12.8 (see § 3.3); notice that the fit is poor in the ($V-I$, V) CMD. We will consider this point later.

The upper main sequence appears composed of a handful of late B-type stars; the brightest of them seem to be slightly evolved. All these stars show moderate scatter in the TCD (B–V, U–B), and have the CMDs that could be produced by non-uniform absorption along the line of sight to the cluster. A group of stars, probably binaries, appear above the ZAMS at $14 \leq V \leq 16$ and the brightest star in our frame, No. 1, is a luminous red star whose membership will be discussed below.

Cluster members are easily segregated from field interloopers for $V \leq 16$ mag by inspecting the location of the stars in all the CMDs and the TCD ($B-V$, $U-B$), simultaneously. Longwards of this magnitude limit, cluster stars merge into the background level and no realistic membership assessment can be made with that method. Nevertheless, membership with acceptable confidence level can still be assigned for faint stars if we adopt the criterion that a star is a non-member when it is more than 1.5 mag above the ZAMS, or just below it. This procedure by no means guarantees that all main sequence will be rejected, but only that their contaminating effect is minimized.

After the membership analysis, a handful of few likely members and several probable cluster members (both shown with filled circles in the figures) are left throughout the main sequence band. Likely members and probable members are indicated in Table 3.

3.2. *Reddening Analysis*

Nine likely members indicated by (*) in Table 3 are of spectral type earlier than about A0, admitting therefore unique reddening solutions in the TCD (B–V, $U-B$). Their individual intrinsic colors, $(B-V)_0$ and $(U-B)_0$, were computed using the standard reddening relations $E_{U-B}/E_{B-V} = 0.72 + 0.05 \times E_{B-V}$ and $(U-B)_0 = 3.69 \times (B-V)_0 + 0.03$ (Vázquez et al. 1995). The resulting mean color excesses were $\langle E_{B-V} \rangle = 0.45 \pm 0.03$ and $\langle E_{U-B} \rangle = 0.33 \pm 0.02$, in good agreement with the previous value $\langle E_{B-V} \rangle = 0.454$ determined by PF88. These mean excess values were applied to the rest of probable cluster members in order to get their respective intrinsic colors.

In terms of the reddening law, $R = A_V/E_{B-V}$, the ($V-I$, V) and ($V-I$, $B-V$) diagrams indicate anomalies in the extinction law. There is a good ZAMS fitting for most of bright stars in the ($V-I$, V) diagram of Fig. 3 (right panel), but it is quite poor among faint stars, as if they were affected by an additional E_{V-I} excess. The ($V-I$, $B-V$) diagram of Fig. 4 (right panel) shows that most of the faint stars do not follow the standard reddening relation $E_{V-I}/E_{B-V} = 1.244$ (Dean, Warren, & Cousins 1978). If cluster stars are affected by normal interstellar absorbing material they should be aligned with the Dean et al. relation, for which $R = A_V/E_{B-V} = 3.1$. The mere inspection of the figure suggests that R should amount to 3.4–3.5 to fit the faint cluster stars also. Unfortunately, since likely cluster members are all included into a very short color excess interval, our data are not suitable to elucidate this problem. In fact, the average of the individual E_{V-I}/E_{B-V} ratios for likely members, derived from the relation between $(V-I)_0$ and $(B-V)_0$ indices (Cousins 1978), yields a mean $\langle E_{V-I} \rangle = 0.58 \pm 0.05$ and then $\langle E_{V-I}/E_{B-V} \rangle = 1.28$, slightly above the normal R-value. First obtaining $(B-V)_0$ from the $U-B$ and $B-V$ fit under the assumption of a "standard reddening law", and then $(V-I)_0$ is justified because, as already demonstrated by Thé & Groot (1983), if R is < 4.1, then the E_{U-B}/E_{B-V} average ratio has the standard value 0.72.

We cautiously adopted $R = 3.1$ to obtain reddening-free magnitudes of members under the form $V_0 = V - 3.1 \times E_{B-V}$. The adopted R and the mean color excess push the mean visual absorption in Lyngå 1 up to $\langle A_V \rangle = 1.4$, in agreement with the absorption limits $1.2 \leq A_V \leq 1.9$ determined in this region by Neckel & Klare (1980).

3.3. *Distance and Age*

The cluster distance modulus was estimated by superimposing the Schmidt-Kaler (1982) ZAMS on the corrected CMDs ($(B-V)_0$, V_0) and ($(U-B)_0$, V_0). The best ZAMS's fitting yielded an absorption-free distance modulus of $V_0 - M_V = 11.40 \pm 0.2$ mag (error from eye-inspection) correspondimg to a distance $d = 1.9 \pm 0.1$ kpc. Though this distance modulus coincides with the one computed by PF88 (11.48 mag), if the R-value is confirmed to be anomalous the cluster could be closer to the Sun.

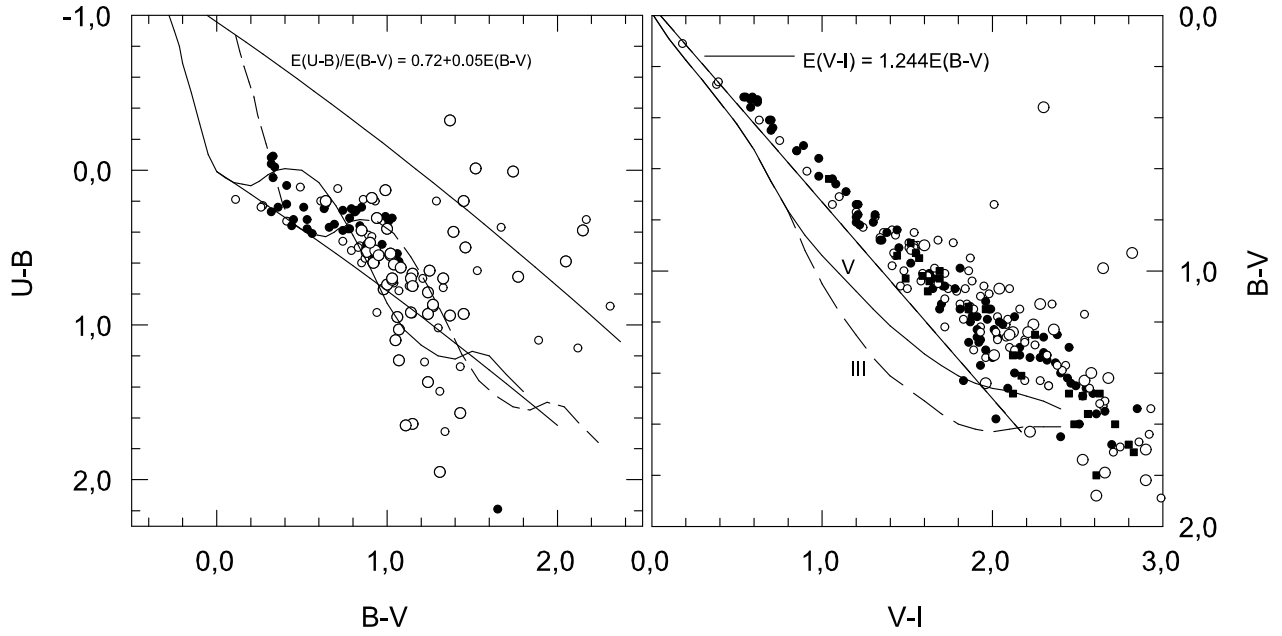

Fig. 4. The TCDs ($B-V$, $U-B$) and ($V-I$, $B-V$). Symbols as in Fig. 2. Solid line in the left panel stands for the intrinsic relation ($B-V$, $U-B$) from Schmidt-Kaler (1982) in its normal position; dashed line is the ZAMS shifted by $E_{B-V} = 0.454$. The path of the reddening line $E_{U-B}/E_{B-V} = 0.72 + 0.05E_{B-V}$ for stars of O and A types is also indicated. In the right panel, solid and dashed lines are the intrinsic color locii for luminosity classes V and III from Cousins (1978). The reddening line from Dean et al. (1978) is also indicated.

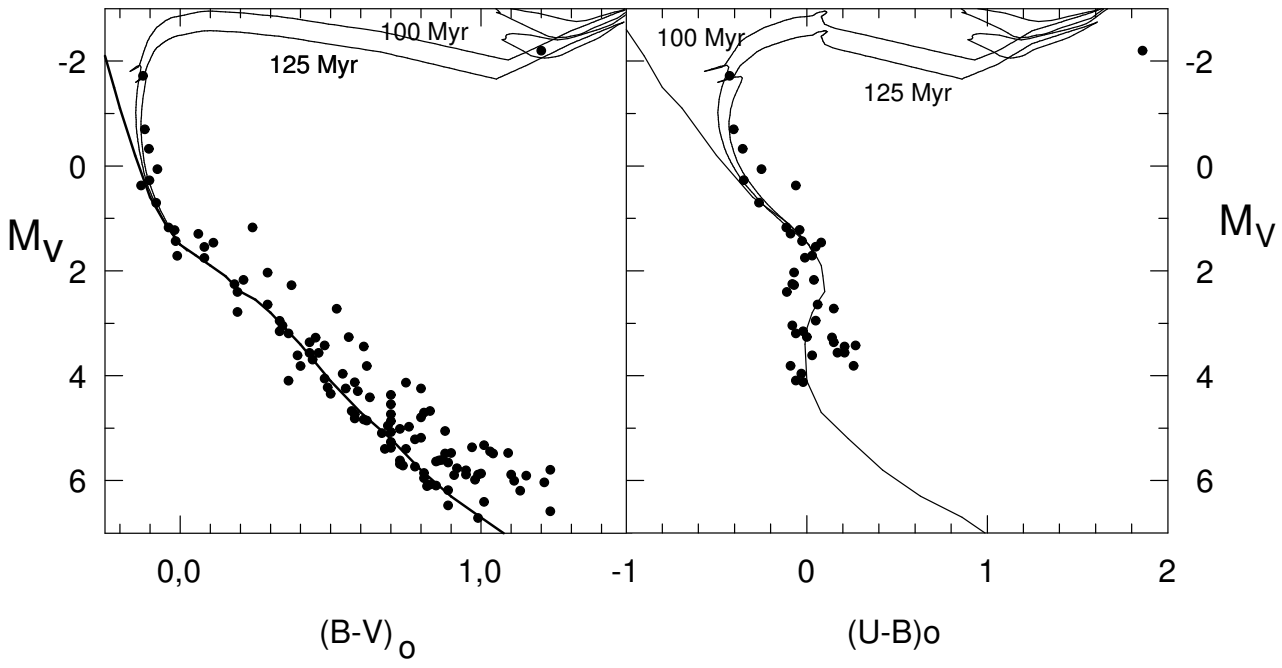

Fig. 5. The ($(B-V)_0$, M_V) and ($(U-B)_0$, M_V) diagrams. Solid lines show the ZAMS (Schmidt-Kaler 1982) fitted to a true distance modulus of 11.40 and the isochrones of Schaller et al. (1992) for ages of 100 and 125 Myr, respectively.

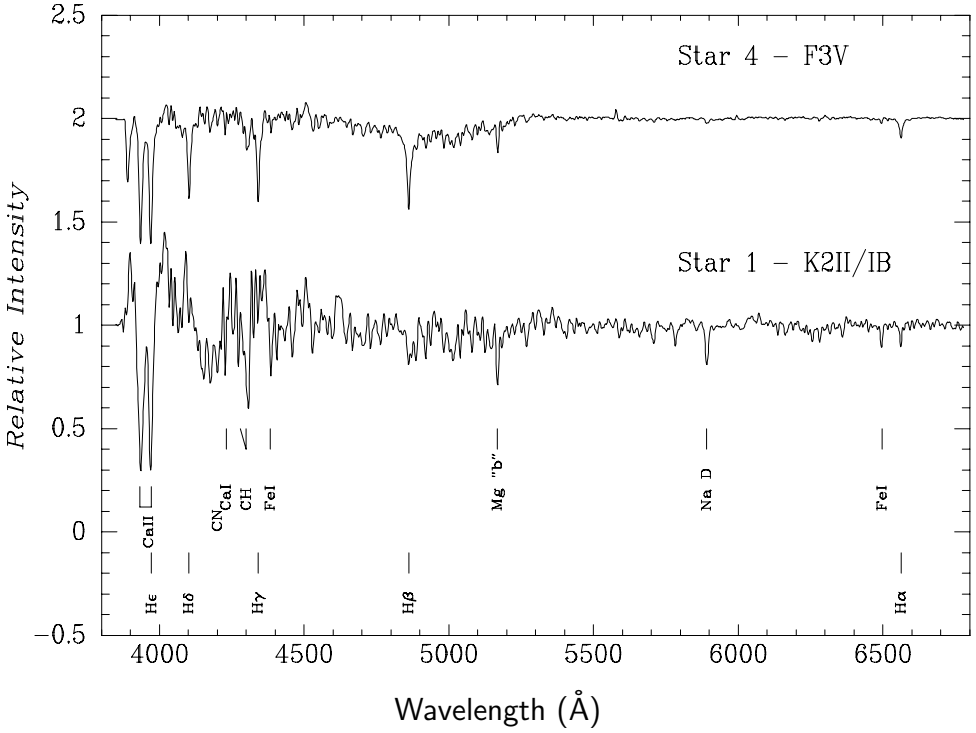

Fig. 6. Observed spectra of stars Nos. 1 and 4.

The age of the cluster was derived by superimposing in the above CMD the isochrones computed from evolutionary models of Schaller et al. (1992) (including mass loss and overshooting, and for solar metallicity). As shown in Figure 5, the best isochrone fitting of the cluster main sequence stars is achieved with the isochrones of 100 and 125 Myr, which fit very well not only the slightly evolved main sequence stars but also the very red star No. 1 (No. 14 in PF88 notation).

Despite the coincidences of our reddening and distance with the values derived by PF88, the cluster age we find here disagrees with the age determined by PF88. They claim that the age of Lyngå 1 is similar to the age of the Pleiades group (about 80 Myr); that is no longer valid with our more extended and deeper data set. We recognize, however, that we could take advantage of evolutionary models (not available to PF88) to perform a more reliable age estimate.

3.4. *Particular Stars*

3.4.1. *Star No. 1*

As it was already mentioned, star No. 1, the brightest one in our sample, is a very red object that, surprisingly, did not receive any further consideration in the PF88 article.

If the observed colors of this star are corrected using the mean reddening values found in § 3.2, and its absolute magnitude is derived using the cluster distance from § 3.3, one obtains: $M_V = -2.22$ mag, $(B-V)_0 = 1.2$, and $(U-B)_0 = 1.85$. These values match reasonably well the expected magnitude and colors for a very luminous star of luminosity class II and spectral type between K0 and K3 (Schmidt-Kaler 1982). Such values also cause star No. 1 to tightly match the cluster isochrones of 100 and 125 Myr in the diagram; probable inaccuracies in the intrinsic $(U-B)_0$ colors of red stars hamper a good fitting on the $((B-V)_0, M_V)$ plane (see Fig. 5). To discard the possibility that star No. 1 is a late-type field star (as most of field stars are: Jones et al. 1981), wrongly considered to be a cluster member, a series of spectra were taken on 2002 February 22/23 using the 215 cm telescope at the CASLEO observatory. The equipment included a REOSC Cassegrain spectrograph and a TeK 1024 × 1024 detector.

The spectral range covered goes from 3300 to 6700 Å at reciprocal dispersion of 85 Å/mm centered in 8°30′ and 11°, respectively. Spectra were reduced using IRAF routines and compared with available atlases (Turnschek et al. 1985; Keenan & McNeil 1976), and with several spectra of stars of types K2 II and K0 II obtained with the same telescope. The analysis of the spectra based in the main spectroscopic fea-

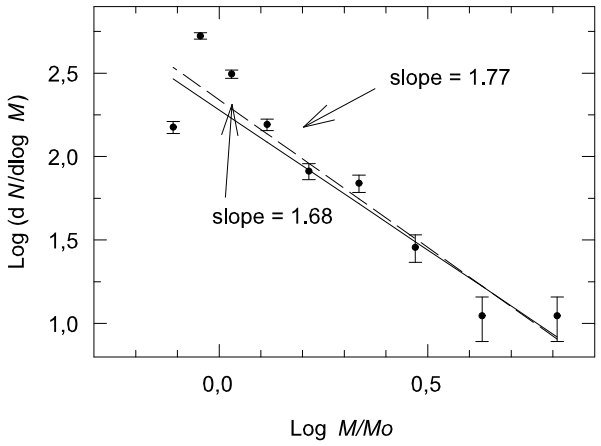

Fig. 7. The present day mass function, PDMF, in Lyngå 1. All mass points but the four less massive were fitted using a least-squares method yielding slopes of $x = 1.77$ and 1.68. See text.

tures shown in Figure 6 indicates that the spectral type of star No. 1 is K2 II–Ib.

In this way, the spectral classification and photometric arguments allow us to consider star No. 1 as a red-supergiant member. Additionally, the proper motions of this star (shown at the bottom of Table 3) $\mu_\alpha \cos\delta = -4.5$ and $\mu_\delta = 2.8$ are, at 1σ, coincident with the average proper motion determined by the 5 stars in the cluster region, $\langle \mu_\alpha \cos\delta \rangle = -9.36 \pm 4.09\,\mathrm{mas\,y^{-1}}$ and $\langle \mu_\delta \rangle = -1.52 \pm 5.5\,\mathrm{mas\,y^{-1}}$.

3.4.2. *Star No. 4*

Spectra were also taken in the same observing run to classify star No. 4 (PF88 20) using the same equipment. This star was considered a reliable cluster member by PF88, but its spectra indicate it is a foreground, less reddened, F3 V star (Fig. 6). Its nature seems to be also confirmed by its large proper motion) compared to the mean of the cluster ($\mu_\alpha \cos\delta = -13.2\,\mathrm{mas\,y^{-1}}$, $\mu_\delta = -10.2\,\mathrm{mas\,y^{-1}}$.

3.5. *Mass Function*

The cluster mass spectrum is defined as the distribution of stars by mass interval. If we assume that all stars in a cluster formed in the same place at a same time, the mass distribution becomes the initial mass function. Lyngå 1 is old enough, and probably some of its most massive stars may have been lost because of evolution. Thus, what we will derive next is, more exactly, the cluster present-day mass function, PDMF.

Following Salpeter (1955), the mass function can be represented by a power law, where the slope of the distribution is given by

$$x = \log(dN/\Delta \log\, M)/\log(M).$$

To get the stellar masses we built first the luminosity function by counting the number of cluster members at each magnitude interval of size $\Delta M_V = 1.0$ mag. The red-supergiant member was included in the brightest interval, as it is assumed to have evolved from a progenitor with at least the same luminosity of the brightest star in the upper main sequence band. The next step was the transformation of each magnitude bin into log(mass) intervals, using the mass-luminosity relation computed by Scalo (1986). Each luminosity bin was given a mean mass according to Scalo (1986) and the number of stars found in them was divided by the corresponding $\Delta \log(\mathrm{mass})$.

As shown in Figure 7, the mass points cover the mass range from 6.5 to $0.8\,M_\odot$, approximately. The figure also shows two different linear fits to the data, which were made using an unweighted least squares method: one of them (dashed line) was obtained rejecting the three faintest mass points, and the other (solid line) was obtained rejecting the four less massive points. Naturally, including all mass points can wrongly increase the slope of the mass spectrum, because of the influence of faint field interlopers not properly removed with the method described in § 3.1. Therefore, to reduce the uncertainty of the probable contamination of field interlopers, the slope of the mass spectrum was computed only in the mass bins indicated above. We obtained slope values $x = 1.77$ and 1.68 respectively, the most probable value beeing $x \approx 1.70 \pm 0.35$. Actually, although a bit large, the present slope value is, at 1σ, still consistent with the Salpeter (1955) value of $x = 1.35$ for field stars. We want to mention that the mass function obtained here belongs to the central part of the cluster, where our photometry covers 90% approximately of the area covered by PF88 photometry (the whole cluster).

A last comment on this topic: Tarrab (1982) established a correspondence between ages and mass function slopes for a sample of open clusters. Inspecting her Table 1, we found that she assigned to clusters about 100 Myr old a mean slope $x = 1.8$, not far from the value we found in Lyngå 1.

4. POLARIZATION MEASUREMENTS

To estimate the amount and direction of the linear polarization towards this object, we obtained *UBVRI* polarimetric measurements in two observational runs on April 30 and May 2, 1998, using the

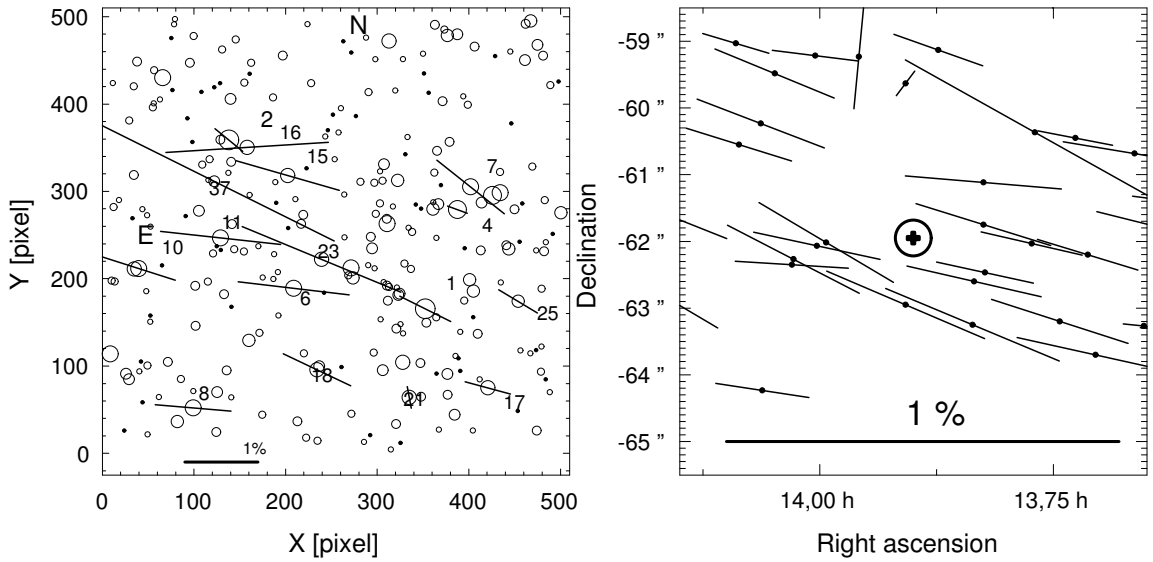

Fig. 8. The polarization vectors in the V filter in Lyngå 1 [this work, left panel] and from Klare & Neckel (1976) in a region $7^\circ \times 7^\circ$ [right panel] centered on Lyngå 1 indicated by a plus (+) sign enclosed by a circle. Coordinates are for the epoch 1950. The 1% polarization vector is indicated in both pannels.

Torino Observatory Five Channel Photopolarimeter, attached to the 215 cm telescope at the Complejo Astronómico El Leoncito (CASLEO). The observations were made with a $15''$ diameter diaphragm and a set of filters having effective wavelengths, $\lambda_U = 0.360\,\mu$m, $\lambda_B = 0.440\,\mu$m, $\lambda_V = 0.530\,\mu$m, $\lambda_R = 0.690\,\mu$m, and $\lambda_I = 0.830\,\mu$m. Standard stars of 0% polarization (HD 090589, HD 115617, HD 146233, and HD 68456) from Gliese (1969) and of polarization angle (HD 111613, HD 147084, and HD 187929) from Serkowski, Mathewson, & Ford (1975) were observed each night.

The percentage of polarization P_λ, the position angle θ_λ, the corresponding errors for each filter and the number of observations, n, can be found in Table 4. The polarization uncertainty, ΔP, was computed from photon statistics, while the uncertainty in the polarization angle, $\Delta\theta$, was estimated using Hsu & Breger (1982) equation:

$$\Delta\theta = 28\overset{\circ}{.}65 \times \frac{\Delta P}{P}.$$

The uncertainty in the polarization angle, $\Delta\theta$, shown in Table 4, is a bit larger than usual and, therefore, more polarimetric measures are needed to reduce ΔP and $\Delta\theta$. However, since we are not interested in the individual polarimetric peculiarities of stars but in the global trend of the interstellar medium towards Lyngå 1, the precision achieved in the current work is enough for our purpose.

Since several stars listed in Table 4 show important errors (larger than 15%) in the polarization angles and polarization vectors—that causes our polarimetry to be of restricted utility—we will just perform a preliminary interpretation of the polarimetric data of Lyngå 1 in the V filter (Figure 8, left panel) till new observations of this kind are available. Fig. 8 (right panel) shows the spatial distribution of polarimetry vectors from Klare & Neckel (1976) in a $7^\circ \times 7^\circ$ field around Lyngå 1. The sign (+) enclosed by a circle stands for the location of the cluster. Nothing relevant or unusual is revealed by comparing the polarimetry in the cluster and in the extended area around it. Indeed, the spatial patterns in the area of Lyngå 1 and its outskirts are completely similar, with a marginal trend for cluster stars to show a bit larger polarization values. Excluding stars Nos. 4, 7, 16, 21, 23, 25, and 37 (because of their large errors) the mean percentage of polarization of field stars in the region of Lyngå 1 is $\approx 1.1\%$, similar to the polarization values found for cluster members. This would indicate just a little influence of the interstellar dust associated to the cluster. That agrees with the images of the Digital Sky Survey[5] chart, where no obvious presence of dust clouds in front of the cluster is evident. We warn,

[5]The Digital Sky Surveys were produced at the Space Telescope Science Institute under U.S. Government grant NAG W-2166. The images of these surveys photographic data obtained using the Oschin Schmidt Telescope on Palomar Mountain and the UK Schmidt Telescope. The plates were processed into the present compressed digital form with the permission of these institutions.

however, that all these values should be revised and completed in more extended work, since we detected some evidence of data scatter as shown in Fig. 4 (left panel).

5. CONCLUSIONS

This is the first time that the entire main sequence of the poorly-populated open cluster Lyngå 1 has been observed. Several new cluster members have been detected and its reddening and distance have been confirmed. Although we have assumed that the R value is normal in the cluster area, there is weak evidence that it could amount to 3.5; this could reduce the distance found in this work, which is coincident with the previous value of 1.9 kpc found by PF88. A comparison with modern isochrone sets increases the cluster age up to 100–125 Myr.

Probably the most important result of this work is that the bright red star No. 1, a red-supergiant of spectral type K2 II–I, can be now recognized as a cluster member. Both photometry and spectroscopy, and to some extent, proper motions, confirm membership for star No. 1.

The cluster mass spectrum has a slope $x \approx 1.7$, which fits nicely in the scheme of ages and mean slopes proposed by Tarrab (1982).

Finally, although of low quality, our polarimetry confirms in principle that the interstellar medium properties in the direction to the cluster follow the more general pattern in the Galaxy shown by Neckel & Klare (1976), in both direction and degree of polarization.

R.V. is indebted to Dr. Garrison for allocation of telescope time at UTSO. E.G. and M.B. did this work under a grant from the Comisión de Investigaciones Científicas y Técnicas de la Prov. de Buenos Aires. R.A.V., G.B., and G.R.S. acknowledge the kind assistance of the CASLEO staff and CONICET support. Special thanks are given to our colleague P. Ostrov for obtaining a series of spectra of stars Nos. 1 and 4. Finally, we are indebted to an anonymous referee who helped us with very useful comments.

REFERENCES

Carraro, G., Chiosi, C., Bressan, A., & Bertelli, G. 1994, A&AS, 103, 375
Cousins, A. W. J. 1978, Mon.Notes R.Astron.Soc.S.Afr., 37, 62
Dean, J. F., Warren, P. R.,& Cousins, A. W. J. 1978, MNRAS, 183, 569
ESA 1997, The Hipparcos and Tycho Catalogues, ESA-SP-1200 (ESA: Publ. Div., Noordwijk)
Gliese, W. 1969, Catalogue of Nearby Stars (Heidelberg: Veroffentlichungen des Astronomischen Rechen-Instituts), 22
Grotues, H.-G., & Gocherman, J. 1992, The Messenger, 68, 43
Hron, J. 1987, A&A, 176, 34
Hsu, J. C., & Breger, M. 1982, ApJ, 262, 732
Jones, T. J., Ashley, M., Hyland, A. R., & Ruelas-Mayorga. A. 1981, MNRAS, 197, 413
Keenan, P. C., & McNeil, R. C. 1976, An Atlas of Spectra of Cooler Stars: Types G, K, M,S , and C (Ohio: Ohio State Univ. Press)
Klare, G., & Neckel, Th. 1976, A&A, 52, 77
Neckel, Th. & Klare, G. 1980, A&AS, 42, 251
Peterson, Ch. J., & Fitzgerald, M. P. 1988, MNRAS, 235, 1439
Phelps, R. L., & Janes, K. A. 1993, AJ, 106, 1870
_____. 1994, ApJS, 90, 31
Salpeter, E. E. 1955, ApJ, 121, 161
Scalo, J. 1986, Fund. Cos. Phys., 11, 144
Schaller, G., Schaerer, D., Meynet, G., & Maeder, A. 1992, A&AS, 96
Schmidt-Kaler, Th. 1982, Landolt-Borstein VI/2b
Serkowski, K., Mathewson, D. L., & Ford, V. L. 1975, ApJ, 196, 261
Stetson, P. B. 1987, PASP, 99, 191
Tarrab, J. 1982, A&A, 109, 285
Thé, P. S., & Groot, M. 1983, A&AS, 125, 75
Turnschek, D. E., Turnschek, D. A., Craine, E. R., & Boeshaar, P. C. 1985, An Atlas of Digital Dpectra of Cool Stars, Astronomy and Astrophysics Series V 1 (Tucson, Arizona)
Vázquez, R. A., Baume, G., Feinstein, A., & Prado, P. 1994, A&AS, 116, 75
Vázquez, R. A., Will, J.-M., Prado P., & Feinstein, A. 1995, A&AS, 111, 85

G. Baume, M. A, Brusasco, E. E. Giorgi, G. R. Solivella, and R. A. Vázquez: Observatorio Astronómico de La Plata, Paseo del Bosque s/n, 1900 La Plata, Argentina (rvazquez@fcaglp.fcaglp.unlp.edu.ar).